2006

Vertical Loads Due to Wheat on Obstructions Located on the Floor of a Model Bin

Marek Molenda
Polish Academy of Sciences, Poland

Michael D. Montross
University of Kentucky, michael.montross@uky.edu

Sidney A. Thompson
University of Georgia

Jozef Horabik
Polish Academy of Sciences, Poland

VERTICAL LOADS DUE TO WHEAT ON OBSTRUCTIONS LOCATED ON THE FLOOR OF A MODEL BIN

M. Molenda, M. D. Montross, S. A. Thompson, J. Horabik

ABSTRACT. *Tests were conducted in a model grain bin to evaluate the vertical loads acting on differently shaped obstructions embedded in wheat during filling, detention, and discharge. The bin had corrugated galvanized steel walls with a 1.83 m diameter and a flat bottom. All tests were conducted in a bin that was centrically loaded and unloaded. Three differently shaped obstructions (disc, cone, and cylinder) were tested; each had a circular base equivalent to 6% of the bin floor area. The obstructions were supported in the bin using a three-legged support structure. Each leg of the support structure rested on a load cell attached to the bin floor. Tests were conducted with the obstructions located in the bin at three different eccentricity ratios (ratio of the centerline of the obstruction to the bin radius, ER = 0, 0.5, and 0.67) and at two different grain heights (height of grain depth to bin diameter ratio, H/D = 0.4 and 0.75). The radial distribution of vertical pressures in the bin varied, with the highest pressure in the center of the bin and the lowest at the bin wall. The largest vertical load on the disc and cone obstructions was measured at the end of filling. The largest load on the cylindrical obstruction was observed immediately after the initiation of bin discharge. At the end of filling and detention, the vertical loads on the disc, cone, and cylinder were 4.8, 3.7, and 4.9 kN, respectively, for obstructions located at ER = 0 and H/D = 0.4. At a location closest to the bin wall (ER = 0.67), the vertical loading on the disc, cone, and cylinder were 4.4, 3.4, and 4.4 kN, respectively. The greatest difference in vertical loading between the location and type of obstruction was on the order of 50%. Bending moments were also observed to act on these obstructions. Bending moments at ER = 0.67 were much larger than those determined at ER = 0.5. For the disc and cone, moments at ER = 0.67 were three times as large as those determined for tests conducted at ER = 0.0. At the onset of discharge, the vertical loading on both the disc and cone decreased significantly, while the vertical loading on the cylinder increased significantly. Recommendations based on Eurocode I were used to predict the vertical loading on the disc and cylinder embedded in grain. This technique did an adequate job of predicting the maximum loading on both obstructions within the bin; however, it did not take into account the effect of unloading on the obstruction forces.*

Keywords. *Granular, Internal object, Janssen's equation, Obstructions, Silo.*

During the design of bins, it is normally assumed that stresses are axially symmetric, which is difficult to ensure even in carefully controlled laboratory tests. Unsymmetrical pressure distributions can occur in bins because of many different factors, such as off-center loading or unloading, structural members located within the grain, bin flow devices (CEN, 2003), or even deteriorated grain forming a cohesive solid mass of material attached to the bin wall or floor because of mold or insect problems (Blight, 2004). According to Rotter (1998), the most frequent cause of bin failure is high axial compressive membrane stress caused by unsymmetrical normal wall pressures. Rotter stated that extensive work was needed to accurately quantify the effect of high local stresses.

Tsunakawa and Aoki (1975) measured forces exerted on discs, spheres, and horizontal square bars by flowing bulk solids in model bins with diameters of 5.3 cm and 20.3 cm. An equation with three adjustable parameters was successfully used to compute the force on the obstructions; however, the physical meaning of the parameters was not clear. Zhang et al. (1997) determined loads on a plastic obstruction located at three depths in a 1.0 m diameter model bin. These authors stated that the bin obstruction did not cause significant changes in either static or dynamic pressures in a corrugated steel bin filled with ground feed. Nouguier et al. (2000) analyzed the time evolution of stresses in a noncohesive granular bed cut by the motion of a plane tool. These authors found that the mean force acting on the tool was accurately predicted using an analytical relationship obtained from a limit analysis using Coulomb's failure criterion. However, large force fluctuations were observed in the numerical simulations.

Australian Standard AS 3774 (SAS, 1996) recommends that the vertical force acting on an internal structural element be estimated as the sum of the vertical pressures acting on the plan projected areas and the frictional tractions summed over

Submitted for review in June 2005 as manuscript number SE 5930; approved for publication by the Structures & Environment Division of ASABE in October 2006.

This article is published with the approval of the Director of the Kentucky Agricultural Experiment Station and designated Paper No. 05-05-69.

The authors are **Marek Molenda, ASABE Member Engineer,** Associate Professor, Institute of Agrophysics, Polish Academy of Sciences, Lublin, Poland; **Michael D. Montross, ASABE Member Engineer,** Associate Professor, Department of Biosystems and Agricultural Engineering, University of Kentucky, Lexington Kentucky; **Sidney A. Thompson, ASABE Member Engineer,** Professor, Department of Biological and Agricultural Engineering, University of Georgia, Athens, Georgia; and **Jozef Horabik ASABE Member,** Professor, Institute of Agrophysics, Polish Academy of Sciences, Lublin, Poland. **Corresponding author:** Michael D. Montross, Department of Biosystems and Agricultural Engineering, University of Kentucky, 128 Barnhart Bldg., Lexington, KY 40546-0276; phone: 859-257-3000, ext. 106, fax: 859-257-5671; e-mail: montross@bae.uky.edu.

  ISSN 0001–2351

all projected vertical surfaces. The possibility that friction can act in the same direction on the internal and external surfaces of an internal structural element should be considered (SAS, 1996).

The objectives of this project were: (1) to determine the vertical force on obstructions embedded in grain during static and discharge conditions, and (2) to quantify the degree of asymmetry in the vertical load exerted by grain on obstructions located on the bin floor.

Equipment and Procedures

Tests were conducted in a cylindrical, flat-floor, corrugated-wall steel grain bin. The bin was 1.83 m in diameter and 5.7 m high (a height to diameter ratio, H/D, of 3.1). The wall corrugations were 13 mm high with a period of 67.7 mm. The cylindrical wall of the bin and the flat floor were each supported independently to isolate the wall and floor loads. Both the wall and floor of the model grain bin were each supported by three load cells (accuracy of ±50 N) spaced at an angle of 120° around the circumference of the bin. Soft red winter wheat that was cleaned at a commercial seed facility was used with a moisture content of 11.3% (wet basis) and an uncompacted bulk density of 750 kg/m^3. The bin was centrally filled at a flow rate of approximately 4.4 kg/s using a horizontal conveyor equipped with a discharge spout. After filling, the wheat was allowed to equilibrate during a detention period of 0.5 h. The bin was then discharged through a 7.2 cm diameter discharge orifice located in the center of the bin at a rate of 1800 N/min, which produced a sliding velocity of 3 m/h along the bin wall. The wall and floor loads during loading, detention, and discharge were measured at 1 min intervals until discharge was completed. All tests were conducted using centric filling and centric discharge.

Three obstructions, shaped as a disc, cone, and cylinder, were tested in the model bin at three different radial locations and at two different grain heights. All obstructions were constructed on circular bases with diameters of 0.445 m, which was equivalent to 6% of the bin floor area. The vertex angle of the cone was 60°, and the height of the cylinder was 0.675 m. The circular surfaces of the disc and cylinder were constructed of plywood. The walls of the cylinder and cone were covered with smooth, galvanized steel. The obstructions were supported in the bin using a three-legged support structure. The support structure was made from 25 × 50 mm tubing, which allowed the grain to flow through it, and rested on three load cells, which were attached to the bin floor. The support structure load cells, which measured a maximum capacity of 8900 N with an accuracy of ±5 N, were spaced 120° apart in a circular configuration with a radius of 0.17 m.

Figure 1a shows a top view of the bin geometry and axis system along with the location of the wall load cells and the load cells supporting the obstruction. Abbreviations used in the text are ER for eccentricity ratio, which defines the location of the centerline of the obstruction to the centerline of the bin, LC for a load cell supporting the bin wall, and OC for a load cell supporting the obstruction. Tests were conducted in which the obstruction was located at ER = 0 (along the bin centerline), ER = 0.5 (halfway between the bin centerline and the bin wall, as shown in fig. 1a), and ER = 0.67. At ER = 0, OC1 was located co-linear with LC1, OC2 with LC2, and OC3 with LC3. At ER = 0.5 and 0.67, OC1 was co-linear with LC1, while OC2 and OC3 were located equidistant from the bin wall, as shown in figure 1a. Two different support structures were used during testing with heights of 0.725 m and 1.37 m above the bin floor, which positioned the base of the obstruction at H/D = 0.4 and H/D = 0.75, respectively; a cylindrical obstruction at H/D = 0.4 and ER = 0 is shown in fig–

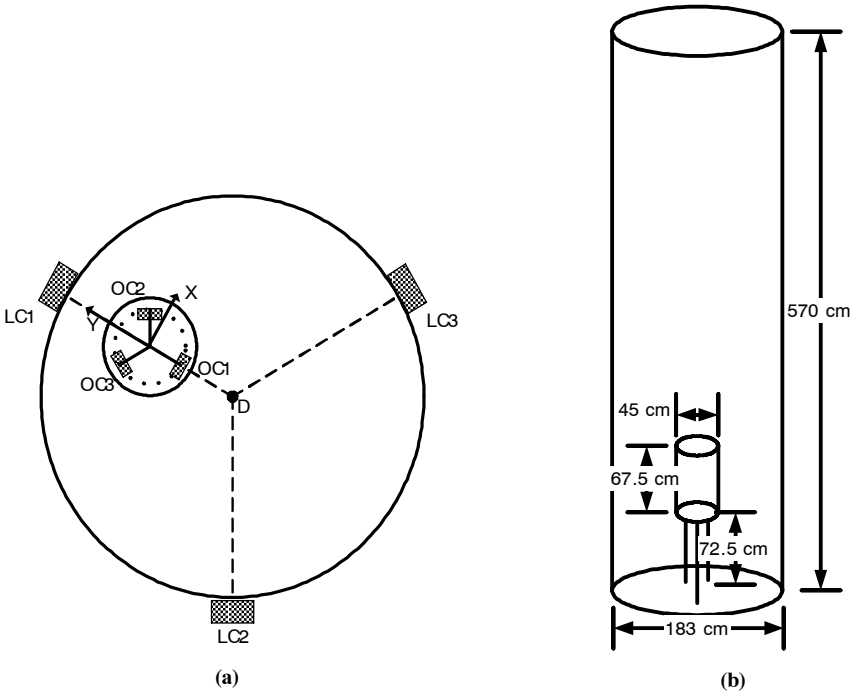

Figure 1. (a) Location of wall load cells (LC), obstruction load cells (OC), and discharge orifice (D) for eccentric obstruction position (ER = 0.5; solid line of the obstruction is the base and dashed line under the obstruction represents the supporting structure), and (b) location of the cylindrical obstruction within the bin at H/D = 0.4 and ER = 0.0.

ure 1b. The X-Y axis system shown in figure 1 was used to calculate the bending moments.

Verification of the load cell accuracy was performed using a water tank mounted on the wall or floor support system. A flowmeter was used to measure the increase in water volume flowing into the tank. Each experimental condition was performed without replication. Previous experiments using the laboratory bins and equipment (Molenda et al., 1996) allowed for the estimation of run-to-run variability as well as its sources. Replications showed that run-to-run variability within the load cells was negligible compared to changes within the experimental protocol. To estimate variability of the load cells supporting the obstruction, initial tests were run in triplicate. For example, at the end of detention with a centrically located cylindrical obstruction at H/D = 0.4, the mean loads on OC1, OC2, and OC3 were 1007, 1650, and 2133 N, respectively. The standard error for the load cells was 40.3 N, more than ten times lower than the differences observed on the obstruction load cells. Previous tests within the facility indicated that the variation in loads over 72 runs resulted in an average wall load to total load ratio at the end of filling of 0.8799, with a standard error of 0.0099 (Day, 2005). In addition, it was found that material properties that influence bin loads (i.e., compressibility of the grain, grain-on-grain friction, and grain-on-steel friction) did not vary significantly during testing. Tests were only repeated when irregular results were obtained due to equipment failures or errors in the test procedure.

Analytical Techniques for Estimating Loads on Obstructions

Australian grain bin standard AS 3774 (SAS, 1996) recommends that the vertical force acting on an internal structural element located within the stored material can be estimated by the sum of the vertical pressures acting on the plan projected areas of the object in addition to the frictional tractional forces summed over all projected vertical surfaces. Motzkus (1974) developed a force balance that led to the determination of the differential vertical force (dV) transmitted by grain onto a wedge-shaped obstruction:

$$dV = (\tan\theta_i + \tan\varphi_x \cdot \lambda_w) \cdot \sigma_{vi} \cdot L \cdot dz_i \quad (1)$$

where

θ_i = half vertex angle of the obstruction
φ_x = wall friction angle
λ_w = ratio of horizontal to vertical stress at the silo wall at the level of the obstruction
σ_{vi} = vertical stress at the level of the obstruction
L = length
z_i = coordinate of the obstruction base in vertical direction.

Eurocode I (CEN, 2003) also suggests an analytical technique for obstructions embedded in granular materials. In this technique, Janssen's equation (Janssen, 1895) is used to predict the pressures that exist over the surface of an obstruction. For determination of the vertical pressure (p_{vf}) at any depth after symmetrical filling, Eurocode 1 (CEN, 2003) recommends:

$$p_{vf}(z) = \frac{p_{h0}}{K} Y_J(z) \quad (2)$$

where

$$p_{h0} = \gamma K z_0 \quad (3)$$

$$z_0 = \frac{1}{K\mu}\frac{A}{U} = \frac{\pi d^2}{4K\mu\pi d} = \frac{d}{4K\mu} \quad (4)$$

$$Y_J(z) = 1 - e^{z/z_0} \quad (5)$$

and

γ = unit weight (kg/m^3)
μ = wall friction coefficient (–)
d = bin diameter (m)
z = obstruction depth below equivalent grain surface (m)
z_o = equivalent grain surface depth (m)
A = cross-sectional area of the silo (m^2)
U = internal perimeter of silo cross-section (m)
K = lateral pressure ratio (–).

Results and Discussion

Vertical Loads for Axial Location of the Obstructions at Two H/D Levels

Characteristics of the vertical forces acting on an obstruction when located in the center of the bin (ER = 0) are shown in figure 2. Forces acting on the differently shaped obstructions and support structures during both filling and discharge are shown for both H/D = 0.4 and H/D = 0.75. The loads shown in figure 2 include both the vertical load that acted on the obstruction and the vertical load that acted on the support structure. Higher static loads were observed at the end of filling for the obstructions located in the bin at H/D = 0.75 (fig. 2a). At H/D = 0.75, the vertical grain pressures acting on the obstruction were less than those acting at H/D = 0.4; however, the forces acting on the support structure would be much larger because of the surface area of the supporting members. The loads acting on the obstructions at H/D = 0.75 were 1.2 to 1.5 times those acting on the obstructions located at H/D = 0.4. At the end of filling, the highest static load (6.2 kN) occurred on a disc located at H/D = 0.75. For both test conditions, the loads acting on the disc and cylinder at the end of filling were approximately the same, while those acting on the cone were approximately 10% lower.

At the onset of discharge, vertical loads on the disc and cone decreased rapidly. For the disc and cone located at a depth of H/D = 0.75, vertical loads between 2 and 3 kN acted on these obstructions, while at H/D = 0.4, vertical loads between 1 and 2 kN were measured. Loads on the disc and cone were similar. Throughout much of unloading, the loads on the disc and cone remained relatively constant despite the decrease in grain height and vertical floor pressures in the bin. For the cylindrical obstruction, a slight increase in vertical load was observed at the onset of discharge, followed by a gradual load decrease with considerable fluctuation as the height of the grain in the bin decreased. The fluctuations were larger when the cylinder was located at H/D = 0.4 (figs. 2b and 2d). The large surface area of the cylinder wall exposed to the horizontal pressure of the wheat probably created much of this loading variation. At the onset of discharge, the switch from static to dynamic loading conditions resulted in an increase in both horizontal pressure and vertical frictional loads on the wall of the cylinder. This resulted in larger loads on the cylinder. The fluctuations in the

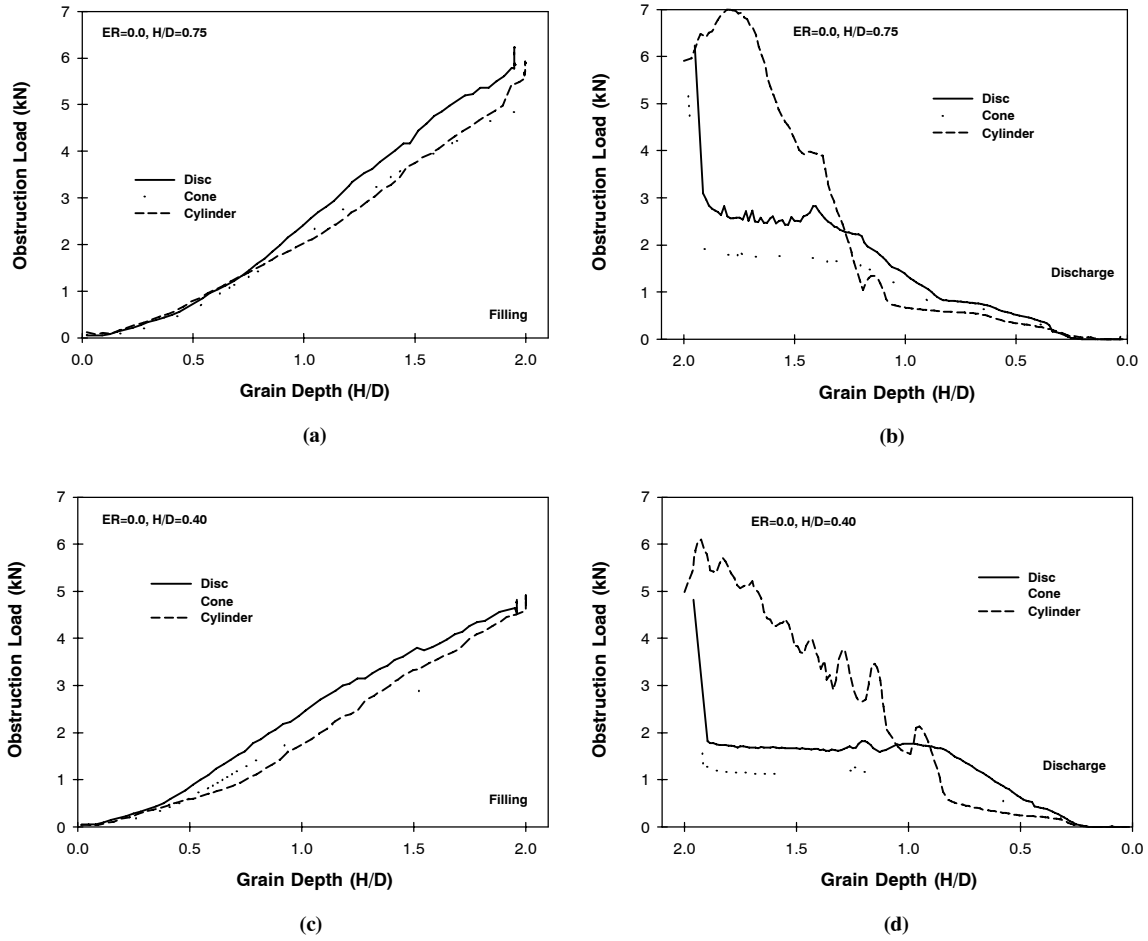

Figure 2. Vertical force on the disc, cone, and cylinder located in the center of the bin (ER = 0) at (a) H/D = 0.75 during filling and detention, (b) at H/D = 0.75 at the end of detention and during discharge, (c) at H/D = 0.4 during filling and detention, and (d) at H/D = 0.4 at the end of detention and during discharge.

loads on the cylinder were thought to originate from changes in the wall frictional force caused by wheat sliding along the cylinder wall.

Asymmetry of Loads for Axial Location of the Obstructions at Two H/D Levels

In figure 3, the loads recorded by the three load cells OC1, OC2, and OC3, which supported the obstruction and support structure, are shown during filling, detention, and centric discharge. This figure shows the loads acting on a cylindrical obstruction, located centrically (ER = 0) at H/D = 0.4 above the bin floor. During filling (fig. 3a), the forces increased smoothly, reaching final values of 2.2, 1.6, and 1.0 kN for OC1, OC2, and OC3, respectively. The twofold difference in vertical force between OC1 and OC3 was attributed to imperfect centric filling of the bin. During filling, the stream of

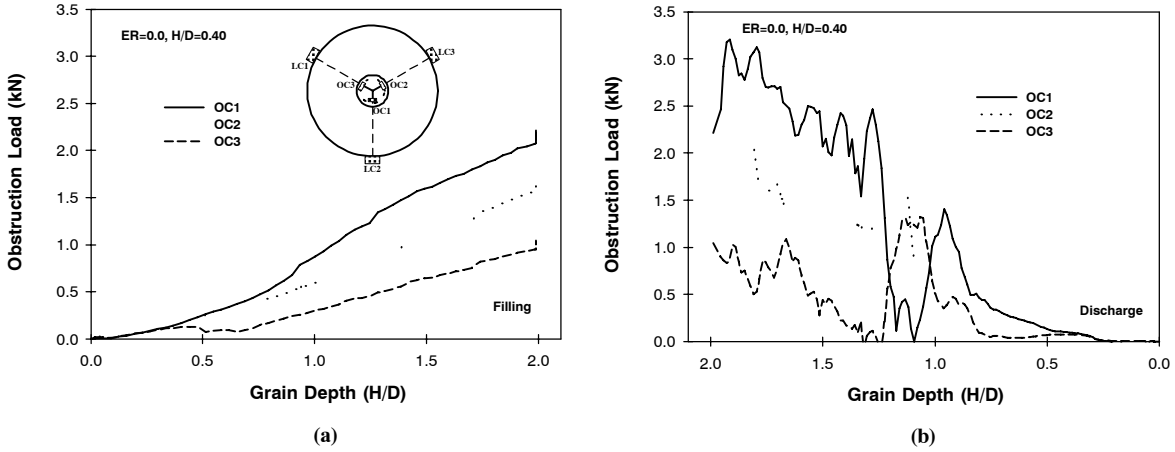

Figure 3. Vertical force on the three load cells supporting the cylinder in the center of the bin (ER = 0) positioned at H/D = 0.4 (a) during filling and detention and (b) at the end of detention and during discharge.

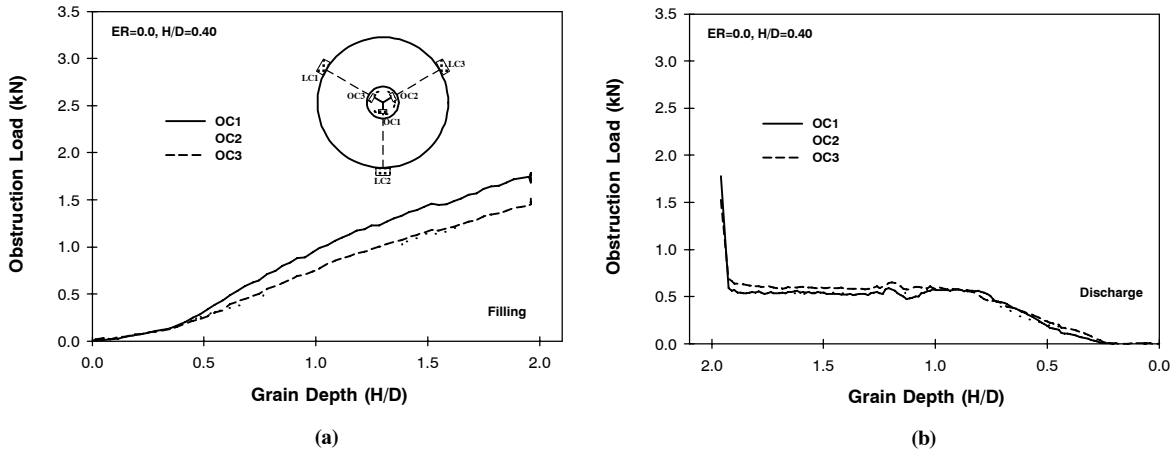

Figure 4. Vertical force on the three load cells supporting the disc in the center of the bin (ER = 0) positioned at H/D = 0.4 (a) during filling and detention and (b) at the end of detention and during discharge.

wheat intercepted the floor surface closest to floor load cell LC1, which was aligned with load cell OC3. While LC1, LC2, and LC3 supported the total floor system, their readings also indicated that asymmetry of loading occurred in the test bin during filling. Load cell LC1 had a vertical force reading 4% greater than load cell LC3, which recorded the lowest force of the three floor load cells. Asymmetry of loading was most conspicuous during initial filling (below H/D = 0.15) before the influence of wall friction became significant. During discharge (fig. 3b), large irregular fluctuations in load were observed on each load cell, particularly during plug flow discharge. These fluctuations were attributed to sliding of grain against the cylinder wall during discharge.

Typical plots for the disc at ER = 0 and H/D = 0.4 are shown in figure 4. Considerable asymmetry with the disc was observed during filling, but in a much smaller range (approx. 5 times smaller maximum difference in OC load cells readings) than in the case of the cylindrical obstruction. At

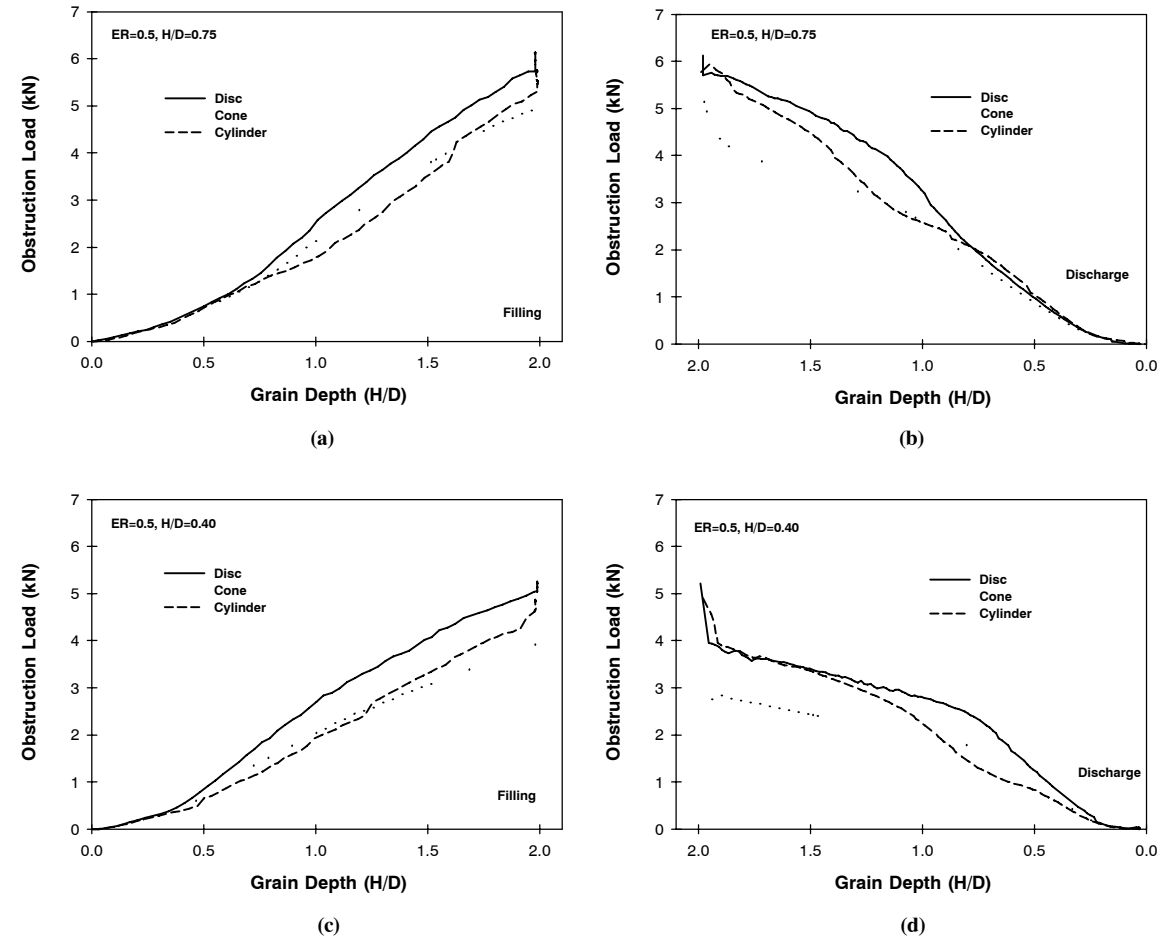

Figure 5. Vertical forces on the disc, cone, and cylinder located at ER = 0.5 and (a) at H/D = 0.75 during filling and detention, (b) at H/D = 0.75 at the end of detention and during discharge, (c) at H/D = 0.40 during filling and detention, and (d) at H/D = 0.40 at the end of detention and during discharge.

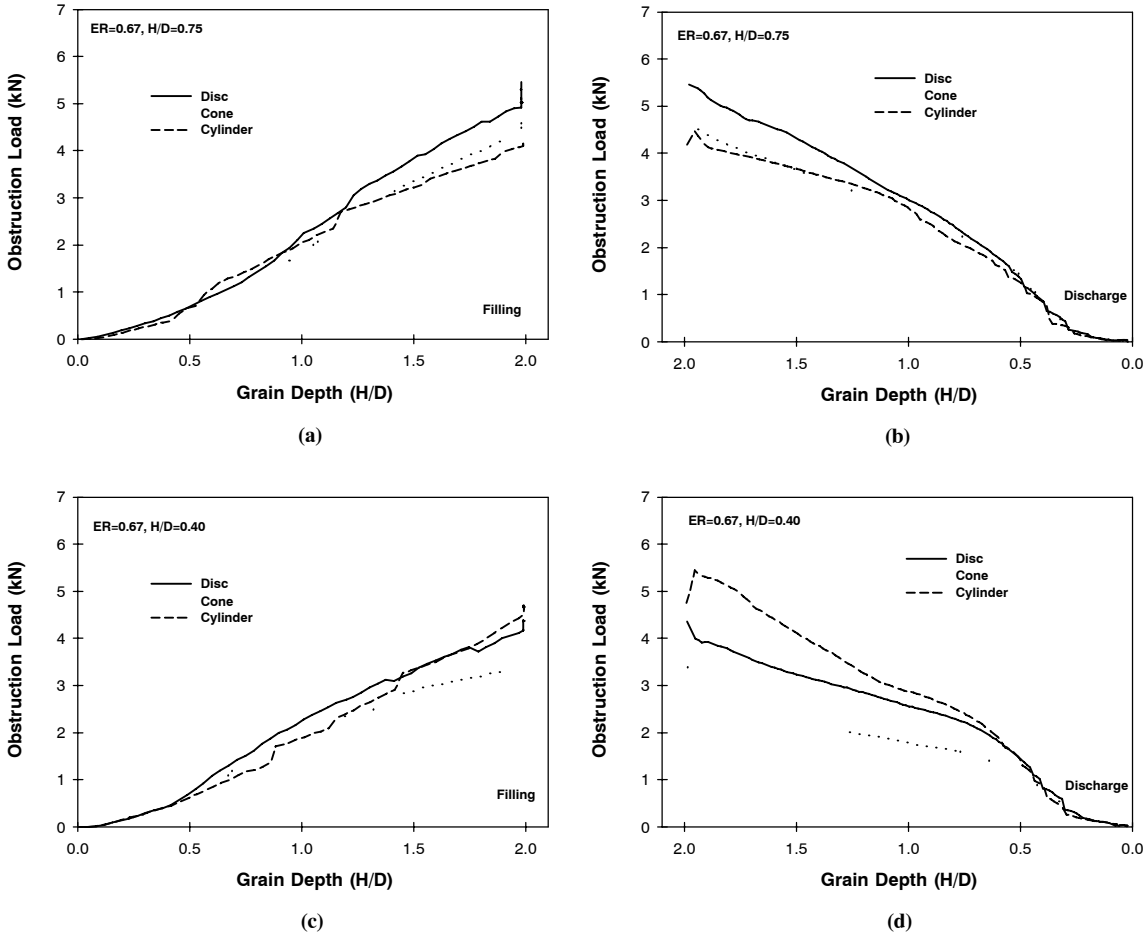

Figure 6. Vertical loads on disc, cone, and cylinder located at ER = 0.67 and (a) at H/D = 0.75 during filling and detention, (b) at H/D = 0.4 during filling and detention, (c) at H/D = 0.75 at the end of detention and during discharge, and (d) at H/D = 0.4 at the end of detention and during discharge.

the onset of discharge, the vertical forces on the disc decreased rapidly to approximately 0.6 kN. During discharge, the loads on each load cell supporting the disc were about the same throughout the test.

Vertical Loads for Non-Axial Location of the Obstructions at Two H/D Levels

Tests were conducted using the three differently shaped obstructions at a radial distance of 0.46 and 0.61 m (ER = 0.5 and ER = 0.67) from the center of the bin at the two different vertical test locations. Vertical loads are shown in figure 5 (ER = 0.5) and figure 6 (ER = 0.67) for both vertical locations. Based on these test results, general trends were observed with respect to both obstruction shape and obstruction location relative to the longitudinal axis of the grain bin. For all static test conditions, the lowest vertical load was always measured on the cone, while the largest vertical load was measured on the disc. The test results also indicated that the vertical pressure was not uniform along the bin radius, but generally decreased with an increased distance from the longitudinal axis of the bin. At H/D = 0.75, the vertical load on the disc varied from 6.2 kN at the center of the bin to 5.5 kN at ER = 0.67. These results demonstrated that the vertical pressure was not uniform across the bin radius, but generally decreased with an increased distance from the bin centerline. This tendency is consistent with results previously reported in the literature (Schwab et al., 1996).

Vertical loads on the disc varied from 4.4 to 6.2 kN and in all cases were larger than the vertical loads that acted on the cone, which varied between 3.4 to 5.7 kN. The vertical loads on the cone were approximately 77% to 90% of the load that acted on the disc when located at the same position. The difference in the loading cannot be attributed only to decreased pressure along the height of the cone, but rather to the effect of a different stress distribution acting on the converging surface of the cone compared to the flat surface of the disc.

Asymmetry of Loads for Non-Axial Location of the Obstructions at Two H/D Levels

Distribution of loads on the three load cells supporting the disc located at H/D = 0.4 and ER = 0.5 is shown in figure 7. Relatively high load asymmetry (compared to the centric location of the disc, fig. 4) was observed while filling the bin, with the lowest force recorded by load cell OC1 nearest the bin centerline (fig. 7a). Approximately equal forces were recorded by the load cells (OC2 and OC3) nearest the bin wall. At the end of filling (fig. 7a), the load on OC1 was 1.2 kN, while values of 2.3 and 2.0 kN were recorded on OC2 and OC3, respectively. This load distribution (with loads on OC2 and OC3 approximately equal, and loads on OC1 approximately half the value) generated a bending moment acting around the axis approximately perpendicular to the bin radius (axis Y in fig. 1). The maximum moment was 225 Nm

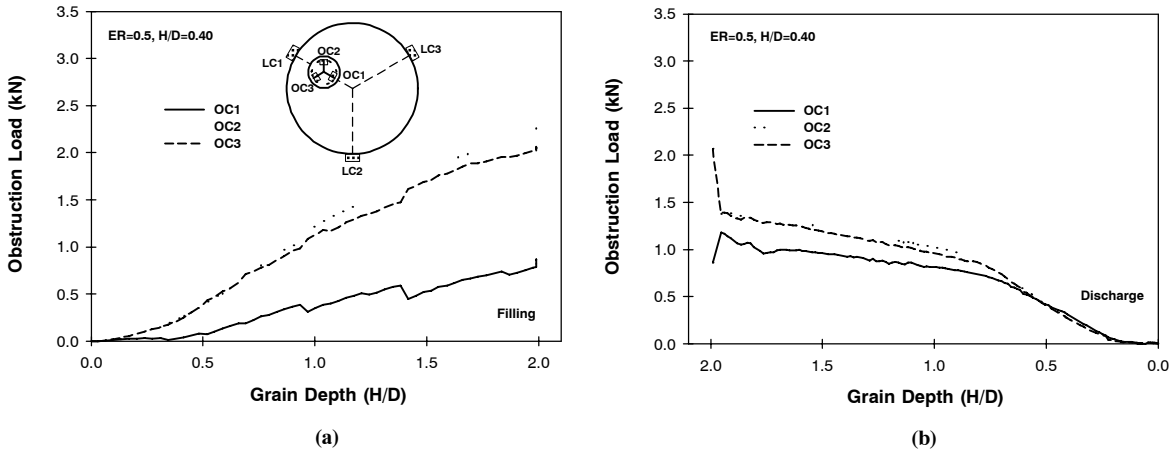

Figure 7. Vertical force on the three load cells supporting the disc at ER = 0.5 and H/D = 0.4 (a) during filling and detention and (b) at the end of detention and during discharge.

at the end of filing. After initiation of discharge, the vertical loads (fig. 7b) and resulting moment rapidly decreased to 37 Nm.

Figure 8 shows the load distribution on the three load cells supporting the cylinder located at H/D = 0.4 and ER = 0.5. Strong load asymmetry was observed on the cylinder. Loads on OC2 and OC3, which were closest to the wall, behaved similarly to the disc. The load on OC2 and OC3 reached a maximum of approximately 2.3 kN at the end of filling, while the load on OC1 did not increase markedly during filling and reached a maximum static value of approximately 0.3 kN (fig. 8a). Upon initiation of discharge (fig. 8b), loads on OC2 and OC3 suddenly decreased to 1.0 and 1.4 kN, respectively, while the load on OC1 ramped up to a value of 1.7 kN. Decreased loads on OC2 and OC3 were a result of decreased vertical loads, which were characteristic of a dynamic stress state. Increased load on OC1 can be attributed to mobilization of friction on the part of the cylinder wall where sliding of grain took place. During further discharge, loads on the cylinder continually decreased without large fluctuations. Maximum resultant moment on the cylinder occurred at the end of filling with a value of 342 Nm, which was approximately 150% of the moment measured on the disc at the same location within the bin. Higher load asymmetry observed with the cylinder was the result of non-uniform lateral pressures and friction forces acting on the cylinder wall. Initiation of discharge caused decreased asymmetry in vertical loads, and the moment ramped down from 342 Nm to 40 Nm. The moments after discharge initiation were similar for the disc and cylinder when they were located in the same region of the bin.

Loads measured on the three load cells supporting the cylinder located closest to the wall (ER = 0.67) and at a higher location (H/D = 0.75) are shown in figure 9. For this location, the loads on OC2 and OC3 followed similar trends and reached values of 2.1 and 2.4 kN, respectively, at the end of filling (fig. 9a). At the onset of discharge, the loads on OC2 and OC3 increased to 2.4 and 2.8 kN, respectively (fig. 9b). The load on OC1 remained close to zero (not higher than 0.13 kN) during the entire cycle of filling and discharge of the bin, which indicated that almost all the load was supported by the two load cells closest to the wall. The moment at the end of detention was 375 Nm and increased to 420 Nm after discharge initiation, which was 25% higher than the moment using the cylinder at ER = 0.5 and H/D = 0.4 (fig. 8). At the higher and more eccentric location of the cylinder, discharge initiation resulted in a slight decrease in the bending moment from 420 Nm to 375 Nm, a decrease in magnitude of 1.1 compared to a 8.5 fold decrease at H/D = 0.4 and ER = 0.5. The maximum bending moments are summarized in figure 10 for all obstructions at all locations within the bin.

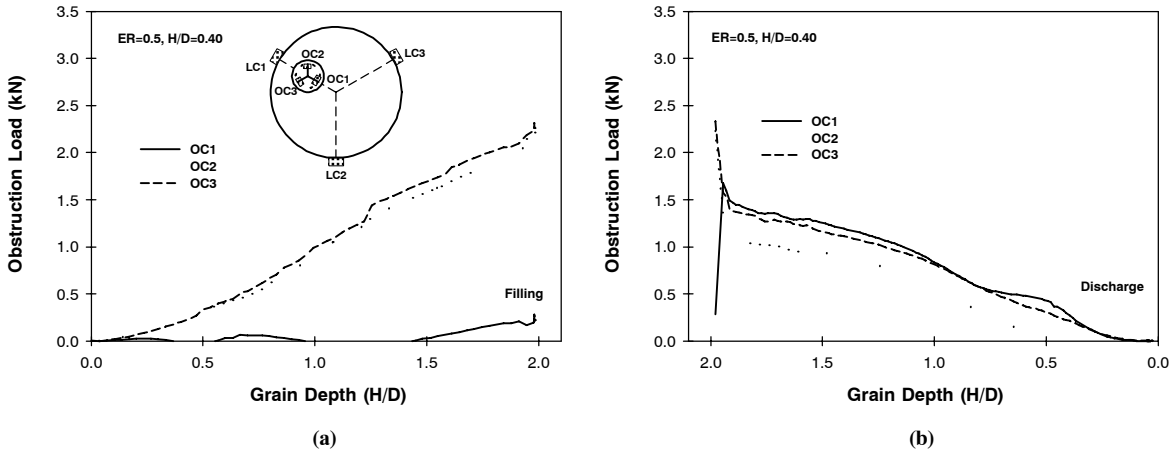

Figure 8. Vertical force on the three load cells supporting the cylinder at ER = 0.5 and H/D = 0.4 (a) during filling and detention and (b) at the end of detention and during discharge.

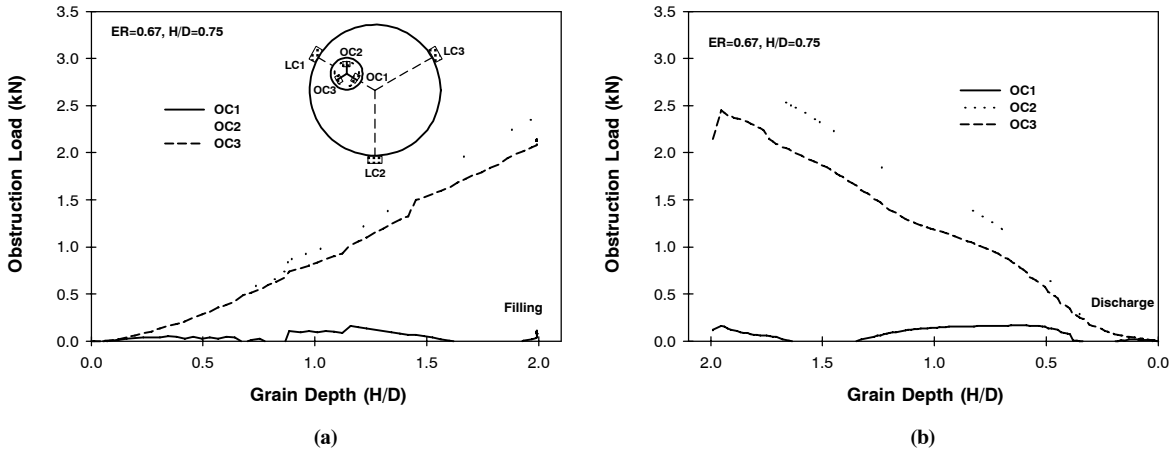

Figure 9. Vertical force on the three load cells supporting the cylinder at ER = 0.67 and H/D = 0.75 (a) during filling and detention and (b) at the end of detention and during discharge.

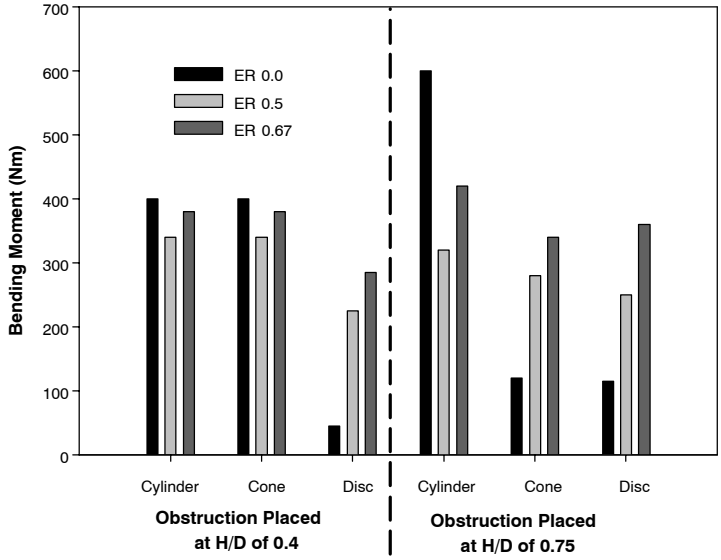

Figure 10. Maximum bending moment (Nm) acting on the disc, cone, and cylinder located at two H/D ratios and three ER values.

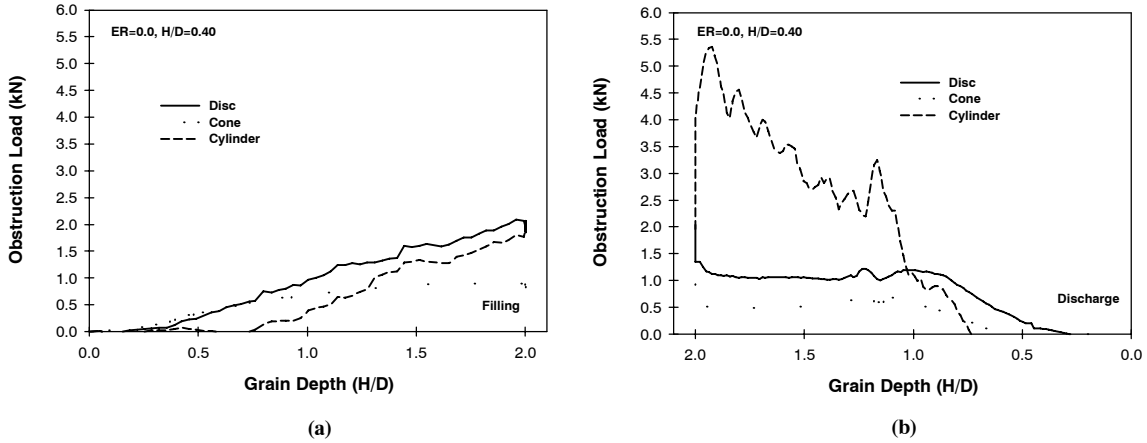

Figure 11. Vertical load on a disc, cone, and cylinder (with the supporting structure load subtracted) located at ER = 0 and H/D = 0.4 (a) during filling and detention and (b) at the end of detention and during discharge.

Estimation of Vertical Obstruction Loads

Corrected Loads

Loads on the obstructions shown in the previous figures contain not only the loads acting on the obstruction located within the grain but also the support structure. To decouple these two effects, a series of experiments was performed in which only the supporting structure was placed in the bin and loaded. These tests showed that the presence of the support

structure introduced an additional static load of 2.8 kN and 3.6 kN for obstructions located at H/D = 0.4 and 0.75, respectively. Loads on the supporting structure with no obstruction were then subtracted from those with both the obstruction and support structure to estimate the loads caused by the obstruction. The vertical loads acting on obstructions shaped like a disc, cone, and cylinder are shown in figure 11. These results are for obstructions located at ER = 0 and H/D = 0.4 with the effects of the supporting structure subtracted from the original experimental data. The original experimental data for the combined loading effect caused by the support structure and obstructions are shown in figures 2c and 2d.

Figure 11a shows the loads during filling on the disc, cone, and cylinder with the support structure load subtracted. At the end of filling, the vertical load on the disc and cylinder were approximately the same with values of 2.0 and 1.9 kN, respectively. The vertical load on the cone was only 0.9 kN. After the initiation of discharge, the vertical loads on the disc and cone decreased (fig. 11b). For these two obstructions, the vertical load remained relatively constant during discharge down to a grain height of H/D = 1.0, after which the load gradually decreased. This decrease in load suggested that for certain conical vertex angles of the obstruction, no dynamic load switch occurred on the obstruction. However, since only two angles were investigated, further testing needs to be conducted to make a conclusive explanation.

Comparison of Experimental Results to Analytical Techniques for Estimating Loads on Obstructions

After discharge initiation, loads on the disc and cone ramped down to 1.1 and 0.5 kN, respectively (fig. 11b), with a decrease in vertical load of 0.8 and 0.2 kN for the disc and cone, respectively, from the end of the detention period to the initiation of discharge. The load on the cylinder increased rapidly, from 1.8 at the end of detention to 5.4 kN after initiation of discharge. Significant load fluctuations on the cylinder occurred during discharge, when sliding grain against the cylinder wall took place. An obstruction shaped like a disc or cone had the maximum vertical load at the end of filling, and initiation of discharge resulted in decreased load. At initiation of discharge, the cylinder had an immediate 2.8 fold increase in vertical load.

The estimated load on a disc from Eurocode 1 (CEN, 2003) and the experimental data on vertical load versus grain height are shown in figure 12. Measured static vertical load was in very good agreement with the load estimated by Janssen's formula, with K = 0.42 and μ = 0.4, less than 1% difference. The value for K was taken from a previous study in the same laboratory (Molenda et al., 1996), and μ was measured using a direct shear apparatus (Molenda et al., 2000).

Vertical loads decreased rapidly at discharge initiation and remained stable during further discharge to H/D = 1.0, despite the decreased grain height and the associated vertical stress. Dynamic values of the vertical load on the disc were distinctly lower because of the stress field switch at initiation of discharge. Usually an active (or static) stress exists during filling a silo, while a passive (or dynamic) stress field develops during discharge. The traditionally used term "active" relates to the case when the higher principal stress (σ_1) is oriented vertically, while a state of stress with the σ_1 oriented horizontally is termed "passive" (Drescher, 1991).

During filling, the estimated static load on the disc was in very good agreement with that estimated using Janssen's equation. During discharge, values of the vertical load on the disc were distinctly smaller than those estimated using Janssen's equation. This variation was believed caused by the stress field switch that occurred at the initiation of discharge. During filling, the stresses within a silo are normally in an "active" state in which the highest principal stress (σ_{p1}) is oriented vertically. During discharge, a "passive" stress field develops in which σ_{p1} is oriented horizontally (Drescher, 1991). This change in stress from an "active" to a "passive" stress state resulted in this decrease in stress on the disc. Janssen's equation does not account for this change in stress state.

Using this technique, the vertical loads on a cone-shaped obstruction should have resulted in vertical loads greater than the loads on the disc. However, in all cases, the load on the disc was greater than the load on the cone. The lower vertical load on the cone was in good agreement with the theoretical development from Motzkus (Strutsch and Schwedes, 1994). Motzkus's equation predicted that the vertical load on a conical obstruction increased with an increase in the vertex angle of the obstruction. However, Motzkus's equation contains three integration constants that are not uniquely defined, and therefore this technique is not suited for design calculations.

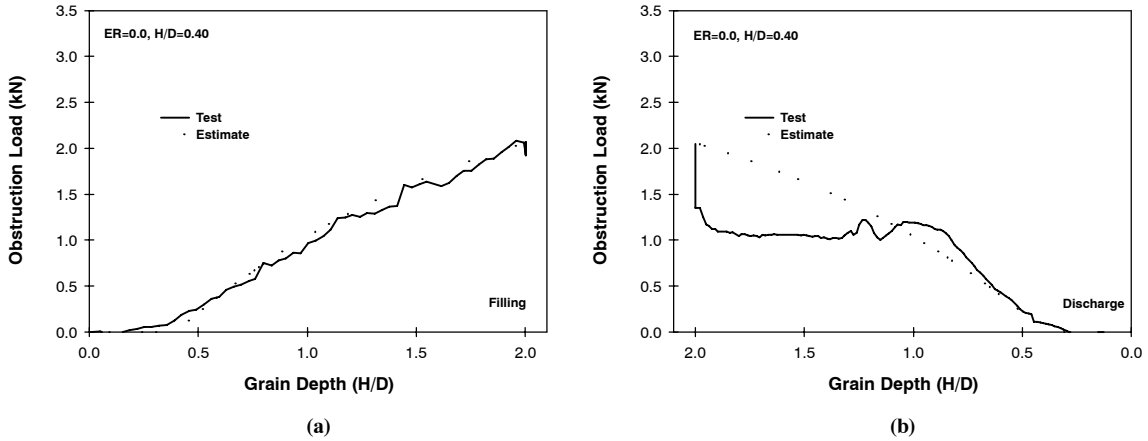

Figure 12. Measured vertical load exerted by grain on the disc at ER= 0.0andH/D = 0.4 and the load estimated using Eurocode 1 with K = 0.42 and μ = 0.4 (a) during filling and detention and (b) at the end of detention and during discharge.

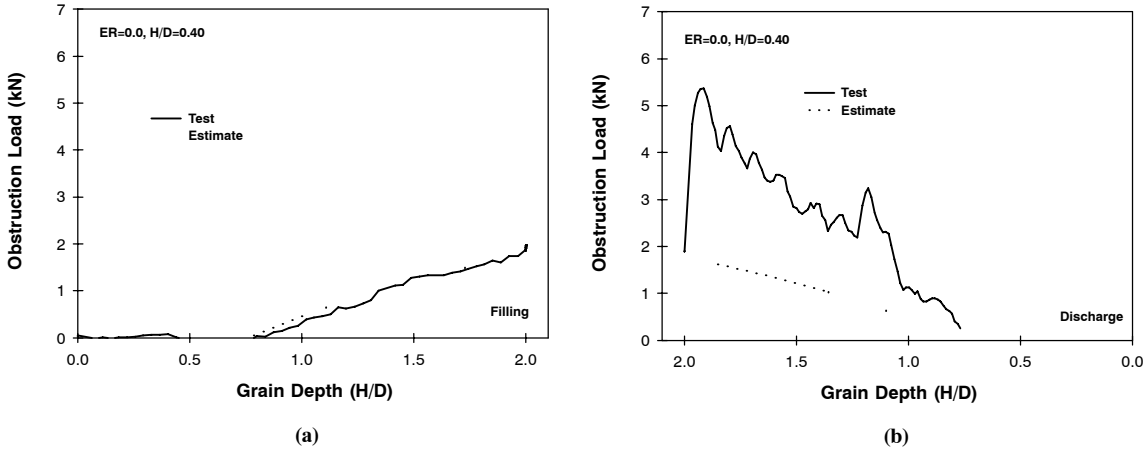

Figure 13. Measured vertical load exerted by grain on the cylinder (with the supporting structure load subtracted) at ER= 0.0andH/D = 0.4 and Eurocode 1 estimates (a) with K = 0.42 and μ = 0.4 (during filling) and (b) with a load magnifying factor of 1.8 (during discharge).

Using Eurocode I (CEN, 2003), the estimated static vertical loads exerted on a cylindrical obstruction were only in good agreement when the stresses acting on only the upper base of the cylinder were considered (fig. 13). When the effects of frictional traction on the walls of the cylinder were taken into account, this resulted in an overestimation of the loads on the obstruction. After filling, frictional forces are oriented in a random manner throughout the bin among individual grains and the bin wall. Therefore, it is believed that friction on the walls of the cylindrical obstruction during filling was not mobilized, and frictional effects were only minor. During discharge (fig. 13b), a large increase in vertical load was observed (1.7 kN to 5.2 kN) immediately after the initiation of discharge. During discharge, the frictional forces assume a more ordered orientation in which the forces act along the centerline of the bin directed along a vector coinciding with the downward grain velocity. This results in higher vertical loads within the bin. The observed increase in vertical load on the cylindrical obstruction was probably a result of both an increased horizontal pressure acting on the obstruction combined with the mobilization of wall friction at the initiation of discharge over the vertical surface of the cylinder. However, this threefold increase in vertical load is higher than any predicted by current design codes. The highest discharge factor recommended by Eurocode I (CEN, 2003) is 1.75 (calculated following clause 5.2.2.1), while ASAE Standard EP 433 (*ASAE Standards*, 2002) recommends an overpressure factor of 1.4 of the static load.

While Janssen's equation provides a simple estimation of the loads that might act on an obstruction embedded in granular materials, this technique fails to include a number of effects that alter the vertical loading of these obstructions. Some of these effects are stress history of the bulk, peak loads at the beginning of discharge, variations in the stress state in the stagnant zone, load asymmetry and load fluctuations, and the non-homogeneity of the material properties originating from variability of the packing structure of the bulk.

Summary and Conclusions

Characteristics of vertical loading on the disc and cone were not distinctly different during both filling and discharge. Initiation of discharge resulted in a sudden drop in vertical load on the cone and disc. The cylindrical obstruction behaved very differently from the disc and cone obstructions. The vertical loading on the cylinder at the initiation of discharge increased, with large fluctuations in vertical loading observed during unloading of the bin.

For eccentrically loaded obstructions, the vertical pressure was lower at the eccentric positions than when located centrically along the axis of the bin. The greatest difference in vertical loading between the location and type of obstruction was on the order of 50%. Bending moments on the obstructions were considerably higher at the eccentric locations for both the disc and cone, while no clear tendencies were observed in the case of the cylinder. For the disc and cone, the moments with the obstruction located at ER = 0.67 were 2.8 times greater than the moments measured at the central location (ER = 0). For the cylinder, no clear tendencies were observed with respect to bending moments.

Current models that predict stresses in grain bins primarily consider only two-dimensional systems with a limited number of rigid particles. No quantitative solution for loads on obstructions within granular materials is currently available. Janssen's equation with the appropriate coefficient of wall friction (μ) and pressure ratio (K) gave a good estimation of the load of the disc and cylinder obstruction on the bin floor during filling and detention. However, even when using Janssen's equation, some decision making was required on how to apply the stresses to each surface of the obstruction. In the case of a cylinder, a significant overestimation of the vertical loading on the obstruction occurred during loading, when frictional effects were assumed to act over the vertical surfaces of the obstruction. During unloading, frictional effects on these surfaces need to be taken into account to better estimate the vertical loading on these obstructions.

Acknowledgements

The authors wish to express their appreciation to the College of Agriculture and the Department of Biosystems and Agricultural Engineering, University of Kentucky, for sponsoring Dr. Molenda's visit, which made the research reported in this article possible.

REFERENCES

ASAE Standards. 2002. EP 433: Loads exerted by free flowing grain on bins. St. Joseph, Mich.: ASAE.

Blight, G. E. 2004. Partial failures of corrugated steel silos storing canola. *Bulk Solids Handling* 24(2): 86-90.

CEN. 2003. Eurocode I: Actions on structures, Part 4: Actions on silos and tanks. Brussels, The Netherlands: European Committee for Standardisation.

Day, G. B. V. 2005. Granular mechanics formulary for soft red winter wheat in corrugated storage bins. PhD diss. Lexington, Ky.: University of Kentucky.

Drescher, A. 1991. *Analytical Methods in Bin-Load Analysis.* Amsterdam, The Netherlands: Elsevier.

Janssen, H. A. 1895. Investigations of pressure of grain in silo (in German). *Verein Deutscher Ingenieure, Zeitschrift (Dusseldorf)* 39: 1045-1049.

Molenda, M, J. Horabik, and I. J. Ross. 1996. Wear-in effects on loads and flow in a smooth-wall bin. *Trans. ASAE* 39(1): 225-231.

Molenda, M, S. A. Thompson, and I. J. Ross. 2000. Friction of wheat on corrugated and smooth galvanized steel surfaces. *J. Agric. Eng. Research* 77(2): 209-219.

Motzkus, U. 1974. Belastung von Siloböden und Auslauftrichtern durch körnige Schüttgüter. Dissertation. Braunschweig, Germany: Technische Universitaet Braunschweig.

Nouguier, C., C. Bohatier, J. J. Moreau, and F. Radjai. 2000. Force fluctuations in a pushed granular material. *Granular Matter* 2(4): 171-178.

Rotter, J. M. 1998. Shell structures: The new European standard and current research needs. *Thin-Walled Structures* 31(1-3): 3-23.

SAS. 1996. Australian Standard AS 3774: Loads on bulk solids containers. Homebush, New South Wales: Standards Association of Australia.

Schwab, C. V., I. J. Ross, G. M. White, and D. G. Colliver. 1996. Wheat loads and vertical pressure distribution in a full-scale bin: Part II. Detention. *Trans. ASAE* 39(3): 1145-1149.

Strutsch, J., and J. Schwedes. 1994.The use of slice element methods for calculating insert loads. *Bulk Solids Handling* 14(3): 505-512.

Tsunakawa, H., and R. Aoki. 1975. The vertical force of bulk solids on objects in bins. *Powder Tech.* 11(3): 237-243.

Zhang, Q., J. I. Bergen, and M. G. Britton. 1997. The effect of a conical bin insert on flow patterns of ground feed in a model bin. *Canadian Agric. Eng.* 39(3): 215-219.